

# **On Roller Charging of Photoreceptors for Electrophotography**

*Inan Chen and Ming-Kai Tse*  
*Quality Engineering Associates, Inc.*  
*755 Middlesex Turnpike, Unit 3, Billerica MA 01821*  
*Tel: 978-528-2034 · Fax: 978-528-2033*  
*e-mail: info@qea.com*  
*URL: www.qea.com*

*Paper presented at the IS&T's NIP21*  
*International Conference on Digital Printing Technologies*  
*September 18-23, 2005, Baltimore, Maryland*

# On Roller Charging of Photoreceptors for Electrophotography

Inan Chen and Ming-Kai Tse  
Quality Engineering Associates (QEA), Inc.  
Burlington, MA/USA

## Abstract

The process of charging photoreceptors with a biased roller is analyzed with a charge transport model that takes into consideration the space charge effects in the semi-insulating overcoat layer of the roller and the non-Ohmic charge injection at layer boundaries. The effects of these transport parameters on the charging performance are examined. Based on the results, an ideal evaluation technique for charging roller performance is suggested.

## Introduction

The first step of electrophotography, i.e. charging the photoreceptor (PR), is achieved either with a corotron with high voltage wire above the PR or with a biased roller in near contact with the PR. The latter technique has the advantages of low ozone emission and compact size. In typical charging rollers, the conductive elastomer (with conductivity  $\sigma \approx 10^{-7}$  S/cm) surrounding the metal shaft is often overcoated with a thinner ( $\approx 100$   $\mu\text{m}$ ) and more resistive layer (with  $\sigma \approx 10^{-10}$  S/cm) to prevent destructive arcing to the PR. The PR is charged by gaseous ions created when electrical breakdown occurs in the air gap between the roller and the PR.

The process of roller charging had been analyzed by several authors.<sup>1-4</sup> The electrical property of the roller was characterized by its resistance. However, it has been known that the roller resistance, determined from closed-circuit constant voltage measurements, can fluctuate from measurements to measurements and from position to position, and are inconsistent with the device performance. Furthermore, the dielectric relaxation (or open-circuit voltage decay) of the roller has been found to deviate significantly from the exponential time dependence expected from the equivalent R-C circuit equation.<sup>5</sup> Such non-Ohmic charge transport phenomenon also occurs in electrostatic transfer of developed toners. This process has recently been analyzed with a charge transport model that takes into consideration the space charge effects in the bulk and non-Ohmic charge injection from the electrodes into semi-insulating receiving media (e.g., intermediate belts and paper).<sup>6</sup> The non-exponential decay of open-circuit voltage on semi-insulators has also been explained by this model as due to non-Ohmic charge injection at the boundaries and/or field dependent charge mobility.<sup>5,7</sup> With the charge mobility in typical semi-insulators as low as  $\mu \ll 10^{-5}$   $\text{cm}^2/\text{Vsec}$ , the transit time required for a charge to move across a layer of thickness  $L \approx 100$   $\mu\text{m}$  in a field  $E \approx 10^5$

V/cm is  $\tau_t = L/\mu E \approx 10^{-2}$  sec. This is of the same order of magnitude or longer than the relaxation time,  $\tau_r = \epsilon/\sigma \approx 10^{-3}$  sec, (with permittivity  $\epsilon \approx 10^{-13}$  F/cm and  $\sigma \approx 10^{-10}$  S/cm). Under this condition,  $\tau_t \gg \tau_r$ , the charge transport is significantly perturbed by the space charge.

In the previous works,<sup>1-4</sup> the time dependence of the process was associated with the rotation of roller and photoreceptor. The charges in the semi-insulating overcoat layer move with a speed  $\mu E \approx 1$  cm/sec, much slower than the mechanical motion of roller ( $\approx 25$  cm/sec at 60 ppm). Thus, the charge transport imposes a larger constraint on the time dependence of the charging process. In this paper, the space-charge transport model is applied to determine the roles of each transport parameter in the charging process.

## Space Charge Transport Model

The configuration at the charging nip is represented by a one-dimensional three-layer system consisting of the semi-insulating roller-coating layer (RC), the grounded photoreceptor (PR), and the air gap, as shown in Fig. 1.

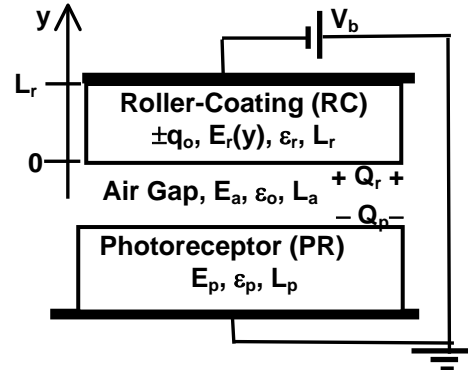


Fig. 1 Schematic of charging nip

Denoting the voltage across the layer  $k$  by  $V_k$ , the field in the layer by  $E_k$ , the layer thickness by  $L_k$ , and the layer permittivity by  $\epsilon_k$ , with the subscript  $k = p, a$  and  $r$  referring to PR, air-gap and RC layers, respectively, and the bias voltage by  $V_b$ , we have,

$$V_p + V_a + V_r = -E_p L_p - E_a L_a + V_r = -V_b \quad (1)$$

The PR and air-gap can be considered space charge free, and hence,  $E_p$  and  $E_a$  are uniform across the respective layer. The space charge in RC layer cannot be neglected, as explained in Introduction. Thus, the field  $E_r(y)$  and the voltage  $V_r$  are expressed in terms of the field  $E_0$  at the

RC/air-gap interface ( $y = 0$ ), and the densities of positive and negative space charge,  $q_p(y)$  and  $q_n(y)$ , respectively, as,

$$E_r(y) = E_{ro} + \int_0^y [q_p(y') + q_n(y')] dy' / \epsilon_r \quad (2a)$$

$$V_r = -\int_0^{L_r} E_r(y) dy = -(E_{ro}L_r + U_r) \quad (2b)$$

with 
$$U_r = \int_0^{L_r} dy \int_0^y [q_p(y') + q_n(y')] dy' / \epsilon_r \quad (2c)$$

Using Gauss theorem, the fields  $E_{ro}$  and  $E_p$  can be related to  $E_a$  and the charges accumulated at the RC/air interface  $Q_r$ , and at the air/PR interface  $Q_p$ , as follows:

$$Q_r = \epsilon_r E_{ro} - \epsilon_a E_a \quad \text{or} \quad E_{ro} = (\epsilon_a E_a + Q_r) / \epsilon_r \quad (3a)$$

$$Q_p = \epsilon_a E_a - \epsilon_p E_p \quad \text{or} \quad E_p = (\epsilon_a E_a - Q_p) / \epsilon_p \quad (3b)$$

Substituting these expressions in Eqs.(1) and (2b), one obtains the air-gap field  $E_a$  as,

$$E_a = (V_b - U_r - Q_r D_r + Q_p D_p) / \epsilon_a \Sigma D \quad (4)$$

where  $D_k = L_k / \epsilon_k$ , (with  $k = p, a, r$ ) and  $\Sigma D$  denotes the sum of three  $D$ 's:  $\Sigma D = L_p / \epsilon_p + L_a / \epsilon_a + L_r / \epsilon_r$ .

At the instant the bias is applied,  $t = 0$ , the interface charges are  $Q_r = Q_p = 0$ . The charge densities in RC are uniform and have the values  $q_p(y) = -q_n(y) = q_i \approx \sigma / \mu$ . Here,  $q_i$  is the intrinsic charge density, related to the conductivity  $\sigma$  and the charge mobility  $\mu$ . Thus, from Eq.(2c),  $U_r = 0$  and the air-gap field is given by Eq.(4) as  $E_a(0) = V_b / \epsilon_a \Sigma D$ . With a small bias voltage  $V_b$ ,  $E_a(0)$  can be less than the air breakdown field  $E_{bk}$ . Let us assume, without loss of generality, that the bias  $V_b > 0$  is applied with the cathode at the roller as illustrated in Fig. 1. Then, as the charge starts to flow in RC (due to dielectric relaxation), negative charges accumulate in RC bulk and at air/RC interface.  $U_r$  and  $Q_r$  begin to have negative values and hence, it can be seen from Eq.(4) that  $E_a$  increases. When  $E_a$  exceeds  $E_{bk}$ , air breakdown creates charge-pairs of an amount  $\pm \delta$ , and  $E_a$  is reduced to  $\leq E_{bk}$ . The PR surface receives the negative charge  $-\delta$  and the counter charge  $+\delta$  is deposited at the air/RC interface. Referring to Eq.(4), this process can be expressed as:

$$Q_p \rightarrow Q_p - \delta \quad \text{and} \quad Q_r \rightarrow Q_r + \delta \quad (5)$$

$$E_a \rightarrow E_{bk} = [V_b - U_r - (Q_r + \delta) D_r + (Q_p - \delta) D_p] / \epsilon_a \Sigma D \quad (6)$$

The amount of charge  $\delta$  can be determined by subtracting Eq.(6) from Eq.(4),

$$\delta = (E_a - E_{bk}) \epsilon_a \Sigma D / (D_r + D_p) \quad (7)$$

After the air breakdown,  $E_a$  is again increased by the charge flow in RC. The air breakdown and the charging of PR are repeated until the increase of (negative)  $Q_p$  can no longer make  $E_a$  to exceed  $E_{bk}$ . Denoting the cumulative sum of air breakdown charge  $\delta$  at each step by  $\Sigma \delta$ , and the total charge supplied to the air/RC interface by the bias voltage through the RC bulk by  $Q_b$ , this condition can be expressed as,

$$Q_p = -\Sigma \delta ; \quad Q_r = Q_b + \Sigma \delta = Q_b - Q_p \quad (8)$$

$$E_a = [V_b - U_r - (Q_b - Q_p) D_r + Q_p D_p] / \epsilon_a \Sigma D \leq E_{bk} \quad (9)$$

Thus, the PR surface charge  $Q_p$  and the open surface voltage of PR,  $V_s$ , are given by,

$$Q_p = -(V_b - U_r - Q_b D_r - \epsilon_a E_{bk} \Sigma D) / (D_r + D_p) \quad (10)$$

$$V_s = |Q_p D_p| \quad (11)$$

It can be seen that the absolute value of  $Q_p$  increases with increasing bias  $V_b$  and injected charges from the bias voltage (negative  $U_r$  and  $Q_b$ ), and a smaller  $E_{bk}$ .

The charge transport in the RC layer is determined by the continuity equations for the positive and negative charge densities,  $q_p(y)$  and  $q_n(y)$ , respectively,<sup>4,5,6</sup>

$$\partial q_k / \partial t = -\partial J_k(y) / \partial y \quad (12)$$

where  $J_k(y) = \mu_k q_k(y) E_r(y)$  is the conduction current, with  $k = p$  and  $n$  for positive and negative charge, respectively. The field  $E_r(y)$  is related to the charge densities  $q_p(y)$  and  $q_n(y)$ , by Poisson's equation, Eq.(2a).

The boundary values of the currents are determined by charge injection from the boundaries at  $y = 0$  and  $L_r$ , and are assumed to be proportional to the local fields,  $E_r(0)$  and  $E_r(L_r)$ , respectively,

$$J_p(0) = s_0 E_r(0) ; \quad J_n(L_r) = s_1 E_r(L_r) \quad (13)$$

where  $s_0$  and  $s_1$  are parameters (with the dimension of conductivity) specifying the injection strength. In addition to deposition of air breakdown charge  $\delta$ , the charge  $Q_r$  at air/RC interface is also changed by the negative current  $J_n$  coming from the bias through the RC layer.

Starting with the initial conditions mentioned above, the charging process is simulated by numerical iteration using these equations. Examples of typical results are presented and discussed in the next section.

## Results and Discussion

The numerical examples are presented in normalized units defined in Table I. The first four basic units are used to

define the next five derived ones. The typical values of the units are chosen for convenience to the present application.

**Table I. Normalized Units**

Units	Typical Values
Length: $L_r$	$10^{-2}$ cm
Permittivity: $\epsilon_a$	$10^{-13}$ F/cm
Charge mobility: $\mu_o$	$3 \times 10^{-5}$ cm <sup>2</sup> /Vsec
Field: $E_{bk}$	$3 \times 10^5$ V/cm
-----	
Time: $t_o = L_r/\mu_o E_{bk}$	$10^{-3}$ sec
Voltage: $V_o = E_{bk} L_r$	$3 \times 10^3$ V
Charge density (volume): $q_o = \epsilon_a E_{bk}/L_r$	$3 \times 10^{-6}$ Coul/cm <sup>3</sup>
Injection strength (and Conductivity) $\sigma_o = \mu_o q_o$	$10^{-10}$ S/cm

Figure 2 shows the time evolution of PR open surface voltage  $V_s$  (Eq. 11) calculated for different bias voltages  $V_b$ . The RC is assumed to have typical values (unity in normalized units) of layer thickness  $L_r$  and charge mobility  $\mu$ . The thickness of air-gap and PR are  $L_a = 0.1$  and  $L_p = 0.2$ , respectively, in units of  $L_r$ . The permittivities are  $\epsilon_r = \epsilon_p = 2.5\epsilon_a$ . The breakdown field  $E_{bk}$  has the unit value (These parameter values are used in all figures below).

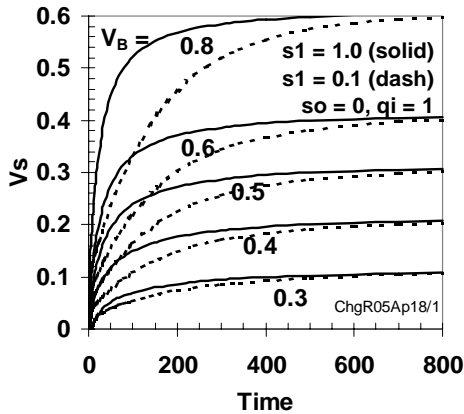


Fig. 2 Time evolution of PR surface voltage  $V_s$ , as the bias  $V_B$  is varied.

In Fig.2, the charge injection from the air-gap is assumed negligible ( $s_o = 0$ ), and two degrees of injection from the bias are considered: a large injection with  $s_1 = 1$  (solid curves) and a small one with  $s_1 = 0.1$  (dashed curves). The intrinsic charge density is  $q_i = 1$ , in normalized units of Table I. It can be seen that with the larger injection,  $V_s$  increases with time to reach the saturation value in about 300 time units ( $t_o$ ). However, with a smaller injection it requires more than 600 $t_o$ . The mobility  $\mu$  is implicit in the time units  $t_o$ .

At a given (long) time,  $V_s$  increases linearly with the bias  $V_b$ , as shown in Fig. 3. With a large injection  $s_1 \geq 1$ , the slope is very close to unity, and the charging requires a threshold bias of  $V_{th} \approx 0.2$ . These features agree with the reported experimental results.<sup>1,2</sup> The linear relation can also be expected from Eqs.(10 and 11). For smaller  $s_1 \approx 0.1$ , the slope is slightly smaller than unity at shorter charging time. The threshold bias is seen to be independent of injection.

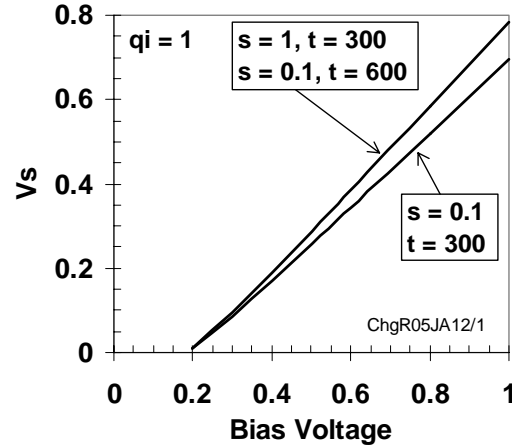


Fig.3 Bias voltage dependence of PR surface voltage  $V_s$ , for injection strength  $s_1 = 1$  and 0.1, at indicated charging time  $t$ .

The features similar to those shown in Figs. 2 and 3 are obtained in calculations with different values of intrinsic charge density  $q_i$ . The relative importance of  $q_i$  and  $s_1$  in the charging process is illustrated by Fig. 4 which shows  $V_s$  at a charging time  $t = 500$ , with a bias  $V_b = 0.5$ , as functions of  $s$ , for various values of  $q_i$ . It can be seen that only for a very large  $q_i \gg 10$ , the charging is insensitive to the injection  $s$ . In semi-insulators,  $q_i$  is more likely smaller, and hence,  $V_s$  can be significantly reduced for  $s \leq 0.1$ , (unless the charging time is much extended).

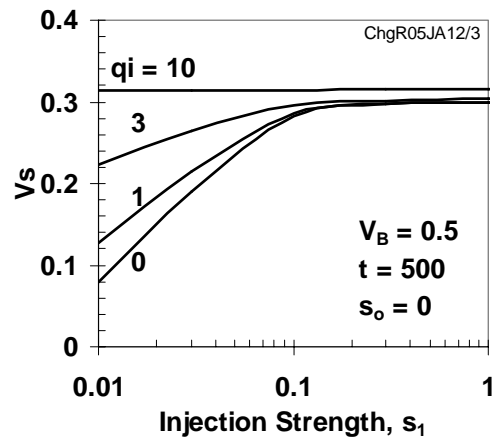


Fig.4 PR surface voltage  $V_s$  vs. injection strength  $s_1$ , for various intrinsic charge density  $q_i$ .

With an AC voltage superimposed on a DC bias, the total bias voltage is given by,  $V_b(t) = V_{dc} + V_{ac}\sin(2\pi\omega t)$ , where  $\omega$  is the frequency of the AC voltage. Figure 5 shows the time evolution of  $V_S$  with a fixed  $V_{dc} = 0.5$  and varying  $V_{ac}$ . The frequency is  $\omega = 1$  (in units of  $1/t_0$ ). At any time  $t$ , the  $V_S$  is seen to increase with increasing  $V_{ac}$  initially, but reverses the trend after  $V_{ac} > 0.6$ . This feature is seen more clearly in Fig. 6, where the asymptotic values (at  $t = 1000$ ) of  $V_S$  are plotted as functions of  $V_{ac}$  for three values of  $V_{dc}$ . The initial rise of  $V_S$  with  $V_{ac}$  is linear, reaching a maximum value very close to  $V_{dc}$ . Independent of the  $V_{dc}$  values, the maximum effect of  $V_{ac}$  occurs at  $V_{ac} \approx 0.6$ . The maximum increase in  $V_S$  due to the added AC equals the threshold voltage  $V_{th}$  ( $\approx 0.2$ ) required in charging with DC bias only (cf. Fig. 3). Thus, with the help of  $V_{ac}$  ( $\approx 0.6$ ),  $V_S$  reaches a value  $\approx V_{dc}$ . The similar results are obtained with other (reasonable) values of  $s$  and/or  $\omega$ . These features are in good agreement with published experimental results.<sup>1,2</sup>

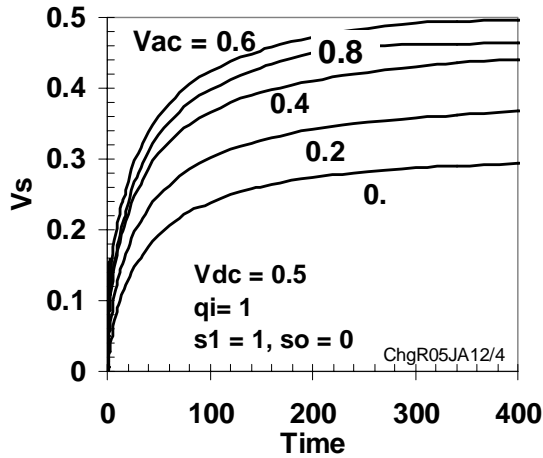


Fig. 5 Time evolutions of  $V_S$  with a fixed  $V_{dc}$  and varying  $V_{ac}$ ,  $q_i$  and  $s$  values indicated.

## Conclusions

With a static one-dimensional geometry, the charge transport model of roller charging has successfully produced many features in good agreement with experimental observations (Figs. 3 and 6). In addition to the process and geometrical parameters such as bias voltage, charging time, layer thickness and permittivity, the model introduced transport parameters of the semi-insulating roller-coating layer, including the intrinsic charge density  $q_i$ , the charge mobility  $\mu$ , and the injection strength  $s$  at the boundaries. The numerical examples have demonstrated that each of the latter parameters plays independently important roles in the charging process. On the other hand, resistivity (or conductivity), used in previous analyses, cannot uniquely reveal the effects of the two components  $q_i$  and  $\mu$ , and hence, is insufficient for the determination of the charging performance.

It is not easy to determine the values of all the parameters,  $q_i$ ,  $\mu$  and  $s$ . Fortunately, these parameters play the same role in open-circuit voltage decays of semi-insulating dielectric layers as in the roller charging process. Based on this correlation, it is suggested that open-circuit voltage decay should be the ideal measurement for evaluation of charging roller performance.<sup>5</sup> The automated and non-destructive technique, known as “Electrostatic Charge Decay” (ECD), has been introduced to perform such tasks.<sup>8</sup>

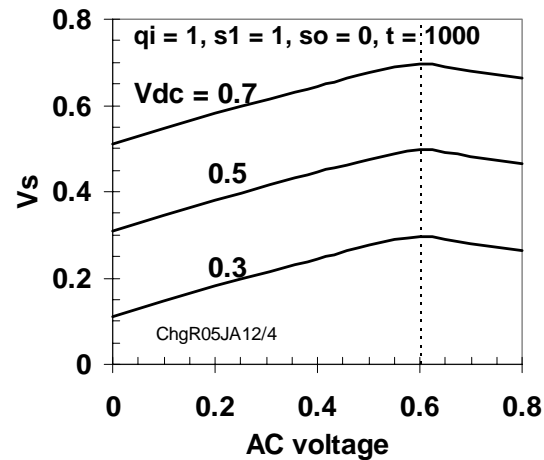


Fig. 6 Asymptotic values of  $V_S$  vs. applied AC bias  $V_{ac}$  for three values of  $V_{dc}$ .

## References

1. S. Nakamura, H. Kisu, J. Araya and K. Okuda, *Electrophotography*, **30**, 302 and 312 (1991)
2. H. Kawamoto and H. Satoh, *J. Imaging Sci. and Technol.* **38**, 383 (1994)
3. M. Kadonaga, T. Katoh and T. Takahashi, *J. Imaging Sci. and Technol.* **43**, 274 (1999)
4. M. Yamamoto, Y. Takuma, K. Kikuchi, and T. Miyasaka, *Proc. IST's NIP-20*, pg.12 (2004)
5. M.-K. Tse and I. Chen, *Proc. IST's NIP-14*, pg. 481 (1998)
6. I. Chen, *Proc. IST's NIP-20*, pg. 30 (2004)
7. I. Chen and M.-K. Tse, *J. Imaging Sci. and Technol.* **44**, 462 (2000)
8. M.-K. Tse, and I. Chen, *Proc. Japan Hardcopy 2005* (in press); M.-K. Tse, D. Forest and F. Y. Wong, *Proc. IS&T's NIP-11*, pg. 383 (1995)

## Author Biography

Inan Chen received his Ph.D. from the University of Michigan in 1964, and worked at Xerox Research Laboratories in Webster, NY, from 1965 to 1998. Currently, he is a consulting scientist for Quality Engineering Associates (QEA), Inc. and others. He specializes in mathematical analyses of physical processes, in particular, those related to electrophotographic technologies. He is the recipient of IS&T's 2005 Chester F. Carlson Award. Contact at inanchen@frontiernet.net or www.qea.com

